Rationalizing Overhauser DNP of nitroxide radicals in water through MD simulations

Supporting Information

Deniz Sezer
Faculty of Engineering and Natural Sciences, Sabancı University, Orhanlı-Tuzla, 34956 Istanbul, Turkey
(Dated: September 29, 2013)

I. METHODS

A. MD simulations

Three separate simulation boxes (one for each temperature) of dimensions specified in Table I were filled with 4001 TIP3P water molecules. Constant-volume MD simulations were performed with NAMD,[1] computing electrostatic interactions with PME.[2] The temperature was controlled with a Langevin thermostat acting on the heavy atoms only. Bonds between heavy and hydrogen atoms were constrained with SHAKE,[3] allowing for an integration time step of 2 fs.

Because the translational diffusion of the solvent molecules plays an essential role for the Overhauser-DNP effect, extra care was taken to ensure that the self-diffusion coefficient of pure water in the MD simulations matches the experimental values given in Table I of the main text. The friction coefficient γ of the Langevin thermostat povides a degree of freedom that can be fine-tuned to this end. At each studied temperature, simulations of pure water with different values of γ were performed and the self-diffusion coefficient was calculated. The simulations were carried for 5 ns. The first one ns was taken as equilibration time and excluded from the analysis. The experimental diffusion coefficients were matched with the γ's specified in Table I. These values were used in the subsequent simulations of TEMPOL, TEMPONE and TEEPOL in water.

One TEMPOL molecule was placed at the center of the box in the final snapshot of the pure water system. Nine water molecules overlapping with TEMPOL were removed, yielding the final system with one nitroxide and 3992 solvent molecules. The same procedure was followed for TEMPONE. Similarly, one TEEPOL molecule was placed in and 12 waters were removed from the pure water system resulting in one nitroxide and 3989 waters. The parameters for the nitroxide TEMPOL were from Ref. 5. The parameters for TEEPOL were obtained by combining the TEMPOL parameters with the existing CHARMM force field.[6] TEMPONE was parametrized following the procedure of Ref. 5. The simulations were carried for 5 ns. The coordinates of the molecules were recorded every 0.2 ps, yielding a total of 25 000 MD frames for the analysis.

To compare with the experimental DNP results at 9.2 T,[7] MD simulations for 1M TEMPOL in water were also carried out. A larger simulation box, with initial $L = 70$ Å, was constructed, which contained 206 TEMPOL molecules and 10215 water molecules. Due to the lack of experimental information about the density of the system in this case, constant pressure simulations were performed for 10 ns. Excluding the first 1 ns from the analysis, average box size was calculated from these constant-pressure simulations, resulting in $L = 71.3758$ Å for the simulation at 35°C. Keeping the size of the simulation volume fixed at that value, additional simulations were carried out for 5 ns. The snapshot in Fig. 7 of the main text is from these constant-volume simulations, which were also used to calculate the RDF in Fig. 8 of the main text.

TABLE I. Water properties matched in the MD simulations containing 4001 water moleculess. The simulation box size (L) was chosen to reproduce the water density (ρ). The friction coefficient of the Langevin thermostat (γ) was calibrated to reproduce the water diffusion coefficient from Table I in the main text.

T	25°C	35°C	45°C
ρ/kg m^{-3}	997[a]	994[a]	990[a]
L/Å	49.3326	49.3822	49.4486
γ/ps^{-1}	11.0	8.7	6.7

[a] Experimental densities from Ref. 4.

B. Spectral densities

The spectral densities deduced from the MD simulations in Eq. (7) of the main text are calculated by taking the spins to be located at their actual positions. To make a connection with the HSCS model we also calculated spectral densities from the MD simulations by taking the spins to be located at the centers of mass of the molecules. For later use, let us introduce the difference between these spectral densities:

$$\delta_{\rm sl}^{\rm MD} \equiv J_{\rm sl}^{\rm MD} - J_{\rm sl,cm}^{\rm MD}. \quad (1)$$

As should be evident from the inset of Fig. 5 of the main text, this difference is actually small—an observation supporting the idea that the HSCS model becomes applicable once the distance between water and TEMPOL falls in the long range region. In terms of $\delta_{\rm sl}^{\rm MD}$ Eq. (7) of the main text can be rewritten as

$$J = J_{\rm ss}^{\rm MD} + 2\delta_{\rm sl}^{\rm MD} + \Delta_{\rm ss} + 2[J_{\rm sl,cm}^{\rm MD} + \Delta_{\rm sl}] + J_{\rm ll}^{\rm HSCS}. \quad (2)$$

The analytical spectral densities in this expression, namely J_x^{abs} and J_x^{HSCS}, depend on the respective HSCS parameters b_x and D_x. As discussed in Sec. III B of the main text, b_{sl} and D_{sl} were determined by fitting $J_{\mathrm{sl}}^{\mathrm{abs}}$ of the absorbing (finite) HSCS model to $J_{\mathrm{sl,cm}}^{\mathrm{MD}}$. Therefore, as a result of the fit, $J_{\mathrm{sl}}^{\mathrm{abs}}(b_{\mathrm{sl}}, D_{\mathrm{sl}}) = J_{\mathrm{sl,cm}}^{\mathrm{MD}}$, which allows us to replace $J_{\mathrm{sl,cm}}^{\mathrm{MD}}$ with the analytical expression. Doing so in (2) and using the definition of Δ_{sl} from Eq. (6) of the main text, leads to

$$J = J_{\mathrm{ss}}^{\mathrm{MD}} + 2\delta_{\mathrm{sl}}^{\mathrm{MD}} + \Delta_{\mathrm{ss}}(b_{\mathrm{ss}}, D_{\mathrm{ss}}) + 2J_{\mathrm{sl}}^{\mathrm{HSCS}}(b_{\mathrm{sl}}, D_{\mathrm{sl}}) + J_{\mathrm{ll}}^{\mathrm{HSCS}}(b_{\mathrm{ll}}, D_{\mathrm{ll}}). \tag{3}$$

The significance of this rewriting is that all the contributions on the second line are available in an analytical form. In contrast, the two contributions on the first line (carrying the MD superscript) need to be calculated numerically from the MD correlation functions. As a result, they are available only on a grid of frequencies determined by the fast Fourier transform routine.

We overcame this inconvenience by calculating the modified correlation function

$$C_{\mathrm{ss,mod}}^{\mathrm{MD}} \equiv C_{\mathrm{ss}}^{\mathrm{MD}} + 2[C_{\mathrm{sl}}^{\mathrm{MD}} - C_{\mathrm{sl,cm}}^{\mathrm{MD}}] \tag{4}$$

from the MD correlation functions. This modified short range-short range correlation function was fitted to a sum of five exponentials:

$$C_{\mathrm{ss,mod}}^{\mathrm{MD}}(\tau) = \sum_{i=1}^{5} a_i \mathrm{e}^{-\tau/\tau_i}. \tag{5}$$

Its Fourer transform was then calculated analytically, yielding an analytical expression for $J_{\mathrm{ss}}^{\mathrm{MD}} + 2\delta_{\mathrm{sl}}^{\mathrm{MD}}$ at any desired frequency ω:

$$J_{\mathrm{ss,mod}}^{\mathrm{MD}}(\omega) = \sum_{i=1}^{5} \frac{a_i \tau_i}{1 + (\omega\tau_i)^2}. \tag{6}$$

In this way, the entire dipolar spectral density J in (3) was available in an analytical form, which was than used to calculate DNP coupling factors at the desired electron and nuclear Larmor frequencies.

Finally, we note that the parameters b_{ll} and D_{ll} needed to calculate $J_{\mathrm{ll}}^{\mathrm{HSCS}}$ in (3) were consistently replaced by b_{sl} and D_{sl} determined from the fits of $J_{\mathrm{sl,cm}}^{\mathrm{MD}}$ by $J_{\mathrm{sl}}^{\mathrm{abs}}$. As discussed in the main text, the parameters b_{ss} and D_{ss} were determined from separate fits of $J_{\mathrm{ss,cm}}^{\mathrm{MD}}$ by $J_{\mathrm{ss}}^{\mathrm{abs}}$. An exhaustive list of the best-fitting parameters b_{ss}, D_{ss}, b_{sl}, D_{sl}, as well as the parameters a_i, τ_i of the exponential fit (5) are given in the next section, which also contains the DNP coupling factors computed using the procedure outlined in the main text of the paper.

II. FITTING PARAMETERS AND COUPLING FACTORS

A. TEMPOL in water

The structure of the free radical TEMPOL is shown in Fig. 1. The parameters determined from the fits of $J^{\mathrm{MD}}_{\mathrm{ss,cm}}$ and $J^{\mathrm{MD}}_{\mathrm{sl,cm}}$ by $J^{\mathrm{abs}}_{\mathrm{ss}}$ and $J^{\mathrm{abs}}_{\mathrm{ss}}$, respectively, are compiled in Table II. Tables III, IV and V contain the amplitudes and times scales of the multi-exponential fits to $C^{\mathrm{MD}}_{\mathrm{ss,mod}}$ [see (5)]. Finally, Table VI gives the calculated coupling factors between TEMPOL and water.

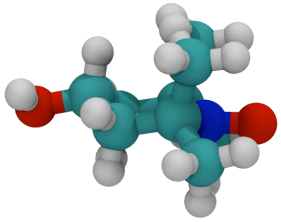

FIG. 1. View of the TEMPOL molecule.

TABLE II. Fitting parameters b (nm) and D ($\mathrm{nm^2ns^{-1}}$) deduced for different choices of the boundaries d and a for TEMPOL in water.

T	d/nm	a/nm	b_{ss}	D_{ss}	b_{sl}	D_{sl}
25°C	1.5	2.45	0.419	2.53	0.433	2.68
	1.8	2.45	0.419	2.56	0.366	2.67
	1.5	2.15	0.419	2.53	0.434	2.70
	1.4	1.95	0.419	2.50	0.412	2.67
35°C	1.5	2.45	0.419	3.13	0.425	3.41
	1.8	2.45	0.424	3.06	0.426	3.34
	1.5	2.15	0.420	3.11	0.426	3.40
	1.4	1.95	0.424	3.02	0.429	3.40
45°C	1.5	2.45	0.420	4.00	0.434	4.28
	1.8	2.45	0.422	4.00	0.432	4.22
	1.5	2.15	0.420	4.00	0.430	4.18
	1.4	1.95	0.420	3.99	0.431	4.15

TABLE III. Time scales (ps) and amplitudes ($\mathrm{nm^{-3}}$) used to fit the modified short range-short range dipolar correlation functions of TEMPOL in water at 25°C.

1.5 - 2.45		1.8 - 24.5		1.5 - 2.15		1.4 - 1.95	
τ_i	a_i	τ_i	a_i	τ_i	a_i	τ_i	a_i
0.139	2.246	0.140	2.230	0.134	2.179	0.131	2.150
1.520	3.938	1.525	3.917	1.409	3.583	1.337	3.358
5.246	4.199	5.270	4.160	4.614	4.206	4.236	4.201
18.97	3.727	18.78	3.604	17.08	3.876	15.71	3.965
70.71	0.375	70.31	0.505	55.26	0.599	45.84	0.776

TABLE IV. Time scales (ps) and amplitudes ($\mathrm{nm^{-3}}$) used to fit the modified short range-short range dipolar correlation functions of TEMPOL in water at 35°C.

1.5 - 2.45		1.8 - 24.5		1.5 - 2.15		1.4 - 1.95	
τ_i	a_i	τ_i	a_i	τ_i	a_i	τ_i	a_i
0.108	1.883	0.108	1.877	0.105	1.851	0.109	1.911
0.796	2.584	0.801	2.580	0.754	2.483	0.800	2.547
3.200	5.244	3.214	5.208	3.081	5.277	3.126	5.147
12.56	3.839	12.48	3.757	11.97	3.877	11.76	3.834
45.06	0.757	47.50	0.850	41.52	0.876	38.11	0.913

TABLE V. Time scales (ps) and amplitudes ($\mathrm{nm^{-3}}$) used to fit the modified short range-short range dipolar correlation functions of TEMPOL in water at 45°C.

1.5 - 2.45		1.8 - 24.5		1.5 - 2.15		1.4 - 1.95	
τ_i	a_i	τ_i	a_i	τ_i	a_i	τ_i	a_i
0.148	2.527	0.148	2.512	0.147	2.512	0.147	2.516
1.210	4.128	1.209	4.104	1.189	4.031	1.185	4.018
4.238	4.467	4.239	4.447	4.050	4.392	4.013	4.344
13.75	2.857	13.53	2.734	12.83	2.866	12.20	2.769
41.11	0.343	41.16	0.495	33.71	0.525	28.11	0.672

TABLE VI. TEMPOL-water coupling factors (%) for the specified ESR frequencies (GHz) calculated for different choices of the boundaries d (nm) and a (nm) with and without finite-size correction (fsc).

	d	a	fsc	9.7	34	94	200	260	330
25°C	1.5	2.45	✓	31.5	15.5	6.03	2.36	1.66	1.21
			-	32.3	16.1	6.27	2.43	1.70	1.23
	1.8	2.45	✓	31.4	15.5	6.02	2.36	1.66	1.21
			-	32.6	16.3	6.35	2.46	1.71	1.24
	1.5	2.15	✓	31.5	15.5	6.03	2.37	1.67	1.22
			-	32.8	16.4	6.40	2.50	1.74	1.26
	1.4	1.95	✓	31.5	15.5	6.02	2.37	1.67	1.22
			-	33.0	16.5	6.46	2.53	1.77	1.28
35°C	1.5	2.45	✓	33.7	18.4	7.47	3.10	2.23	1.64
			-	34.5	19.0	7.77	3.21	2.30	1.67
	1.8	2.45	✓	33.6	18.3	7.44	3.09	2.22	1.63
			-	34.8	19.2	7.86	3.24	2.32	1.69
	1.5	2.15	✓	33.7	18.4	7.48	3.10	2.23	1.64
			-	34.9	19.3	7.93	3.27	2.34	1.71
	1.4	1.95	✓	33.7	18.4	7.47	3.10	2.22	1.63
			-	35.2	19.5	8.01	3.31	2.37	1.73
45°C	1.5	2.45	✓	36.6	21.9	9.83	4.28	3.08	2.28
			-	37.4	22.6	10.2	4.45	3.18	2.34
	1.8	2.45	✓	36.5	21.8	9.81	4.28	3.07	2.27
			-	37.7	22.9	10.4	4.51	3.22	2.37
	1.5	2.15	✓	36.4	21.7	9.77	4.26	3.06	2.26
			-	37.7	22.8	10.4	4.52	3.24	2.38
	1.4	1.95	✓	36.4	21.7	9.74	4.25	3.06	2.26
			-	37.9	23.0	10.5	4.56	3.27	2.41

B. TEMPONE in water

The structure of TEMPONE is in Fig. 2. The parameters determined from the fits of $J^{\rm MD}_{\rm ss,cm}$ and $J^{\rm MD}_{\rm sl,cm}$ by $J^{\rm abs}_{\rm ss}$ and $J^{\rm abs}_{\rm ss}$, respectively, are given Table VII. Table VIII lists the amplitudes and times scales of the multi-exponential fits to $C^{\rm MD}_{\rm ss,mod}$. Table IX gives the calculated coupling factors between TEMPONE and water at 25°C.

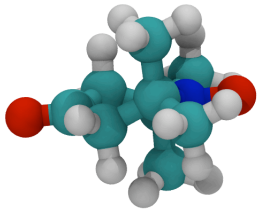

FIG. 2. View of the TEMPONE molecule.

TABLE VII. Fitting parameters b (nm) and D ($\rm nm^2ns^{-1}$) deduced for different choices of the boundaries d and a for TEMPONE in water at 25°C.

d/nm	a/nm	$b_{\rm ss}$	$D_{\rm ss}$	$b_{\rm sl}$	$D_{\rm sl}$
1.5	2.45	0.422	2.55	0.426	2.71
1.8	2.45	0.422	2.58	0.332	2.73
1.5	2.15	0.422	2.56	0.427	2.74
1.4	1.95	0.420	2.56	0.426	2.72

TABLE VIII. Time scales (ps) and amplitudes ($\rm nm^{-3}$) used to fit the modified short range-short range dipolar correlation functions of TEMPONE.

1.5 - 2.45		1.8 - 24.5		1.5 - 2.15		1.4 - 1.95	
τ_i	a_i	τ_i	a_i	τ_i	a_i	τ_i	a_i
0.134	2.086	0.134	2.070	0.134	2.074	0.134	2.081
1.293	3.495	1.292	3.468	1.275	3.411	1.276	3.413
4.956	4.327	4.954	4.295	4.857	4.386	4.818	4.377
18.62	3.707	18.39	3.598	18.48	3.659	18.23	3.659
68.27	0.349	68.05	0.480	62.12	0.397	54.49	0.405

TABLE IX. TEMPONE-water coupling factors (%) for the specified ESR frequencies (GHz) calculated for different choices of the boundaries d (nm) and a (nm) with and without finite-size correction (fsc).

d	a	fsc	9.7	34	94	200	260	330
1.5	2.45	✓	31.6	15.5	5.98	2.43	1.72	1.26
		-	32.5	16.1	6.22	2.51	1.76	1.28
1.8	2.45	✓	31.6	15.5	5.97	2.43	1.72	1.26
		-	32.9	16.3	6.32	2.54	1.78	1.29
1.5	2.15	✓	31.6	15.5	5.97	2.43	1.72	1.26
		-	32.8	16.4	6.35	2.56	1.80	1.31
1.4	1.95	✓	31.5	15.5	5.98	2.43	1.72	1.26
		-	33.0	16.5	6.44	2.60	1.83	1.33

C. TEEPOL in water

The structure of TEEPOL in Fig. 3 shows the larger protecting groups of this radical compared to TEMPOL. The parameters determined from the fits of $J^{\mathrm{MD}}_{\mathrm{ss,cm}}$ and $J^{\mathrm{MD}}_{\mathrm{sl,cm}}$ by $J^{\mathrm{abs}}_{\mathrm{ss}}$ and $J^{\mathrm{abs}}_{\mathrm{ss}}$, respectively, are given Table X. Table XI lists the amplitudes and times scales of the multi-exponential fits to $C^{\mathrm{MD}}_{\mathrm{ss,mod}}$. Table XII gives the calculated coupling factors between TEEPOL and water at 25°C.

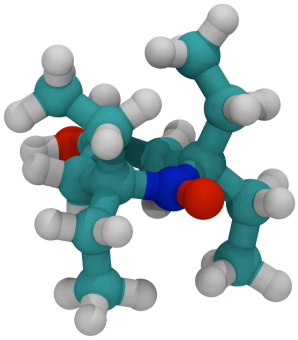

FIG. 3. View of the TEEPOL molecule.

TABLE X. Fitting parameters b (nm) and D ($\mathrm{nm^2ns^{-1}}$) deduced for different choices of the boundaries d and a for TEEPOL in water at 25°C.

d/nm	a/nm	b_{ss}	D_{ss}	b_{sl}	D_{sl}
1.5	2.45	0.452	2.42	0.441	2.53
1.8	2.45	0.453	2.44	0.322	2.57
1.5	2.15	0.450	2.44	0.424	2.59
1.4	1.95	0.450	2.42	0.426	2.60

TABLE XI. Time scales (ps) and amplitudes ($\mathrm{nm^{-3}}$) used to fit the modified short range-short range dipolar correlation functions of TEEPOL.

1.5 - 2.45		1.8 - 24.5		1.5 - 2.15		1.4 - 1.95	
τ_i	a_i	τ_i	a_i	τ_i	a_i	τ_i	a_i
0.091	1.319	0.093	1.334	0.087	1.261	0.080	1.186
0.483	1.206	0.500	1.195	0.450	1.202	0.405	1.234
2.657	4.596	2.680	4.562	2.595	4.530	2.539	4.540
12.58	4.273	12.63	4.228	12.10	4.239	11.68	4.256
48.66	1.121	52.83	1.154	45.91	1.228	42.12	1.308

TABLE XII. TEEPOL-water coupling factors (%) for the specified ESR frequencies (GHz) calculated for different choices of the boundaries d (nm) and a (nm) with and without finite-size correction (fsc).

d	a	fsc	9.7	34	94	200	260	330
1.5	2.45	✓	29.8	13.9	5.16	1.95	1.39	1.03
		-	30.7	14.5	5.38	2.01	1.43	1.05
1.8	2.45	✓	29.9	14.0	5.16	1.95	1.39	1.03
		-	31.1	14.8	5.48	2.04	1.44	1.06
1.5	2.15	✓	29.8	13.9	5.16	1.95	1.39	1.03
		-	31.1	14.8	5.50	2.05	1.45	1.07
1.4	1.95	✓	29.9	14.0	5.18	1.94	1.38	1.03
		-	31.4	15.0	5.58	2.08	1.47	1.08

[1] J. C. Phillips, R. Braun, W. Wang, J. Gumbart, E. Tajkorshid, E. Villa, C. Chipot, R. D. Skeel, L. Kale, and K. Schulten, J. Comp. Chem. **26**, 1781 (2005).
[2] U. Essmann, L. Perera, M. L. Berkowitz, T. Darden, H. Lee, and L. G. Pedersen, J. Chem. Phys. **103**, 8577 (1995).
[3] J.-P. Ryckaert, G. Ciccotti, and H. J. C. Berendsen, J. Comp. Phys. **23**, 327 (1977).
[4] J. Kestin, M. Sokolov, and W. A. Wakeham, J. Phys. Chem. Ref. Data **7**, 941 (1978).
[5] D. Sezer, J. H. Freed, and B. Roux, J. Phys. Chem. B **112**, 5755 (2008).
[6] A. D. MacKerell, D. Bashford, Bellott, R. L. Dunbrack, J. D. Evanseck, M. J. Field, S. Fischer, J. Gao, H. Guo, S. Ha, D. Joseph-McCarthy, L. Kuchnir, K. Kuczera, F. T. K. Lau, C. Mattos, S. Michnick, T. Ngo, D. T. Nguyen, B. Prodhom, W. E. Reiher, B. Roux, M. Schlenkrich, J. C. Smith, R. Stote, J. Straub, M. Watanabe, J. Wiórkiewicz-Kuczera, D. Yin, and M. Karplus, J. Phys. Chem. B **102**, 3586 (1998).
[7] P. Neugebauer, J. G. Krummenacker, V. P. Denysenkov, G. Parigi, C. Luchinat, and T. F. Prisner, Phys. Chem. Chem. Phys. **15**, 6049 (2013).